



LAWRENCE
LIVERMORE
NATIONAL
LABORATORY

Automated alignment of the Advanced Radiographic Capability (ARC) - Target Area at the National Ignition Facility

R. S. Roberts, A. S. Awwal, E. S. Bliss, J. E. Heebner,
R. R. Leach, C. D. Orth, M. C. Rushford, R. R.
Lowe-Webb, K. Wilhelmsen

July 14, 2015

SPIE Optics and Photonics
San Diego, CA, United States
August 9, 2015 through August 13, 2015

Disclaimer

This document was prepared as an account of work sponsored by an agency of the United States government. Neither the United States government nor Lawrence Livermore National Security, LLC, nor any of their employees makes any warranty, expressed or implied, or assumes any legal liability or responsibility for the accuracy, completeness, or usefulness of any information, apparatus, product, or process disclosed, or represents that its use would not infringe privately owned rights. Reference herein to any specific commercial product, process, or service by trade name, trademark, manufacturer, or otherwise does not necessarily constitute or imply its endorsement, recommendation, or favoring by the United States government or Lawrence Livermore National Security, LLC. The views and opinions of authors expressed herein do not necessarily state or reflect those of the United States government or Lawrence Livermore National Security, LLC, and shall not be used for advertising or product endorsement purposes.

Automated alignment of the Advanced Radiographic Capability(ARC)-Target Area at the National Ignition Facility

Randy S. Roberts, Abdul A. S. Awwal, Erlan S. Bliss, John E. Heebner, Richard R. Leach Jr., Charles D. Orth, Michael C. Rushford, Roger R. Lowe-Webb and Karl C. Wilhelmsen

National Ignition Facility,
Lawrence Livermore National Laboratory
Livermore, CA 94551

ABSTRACT

The Advanced Radiographic Capability (ARC) at the National Ignition Facility (NIF) is a petawatt-class, short-pulse laser system designed to provide x-ray backlighting of NIF targets. ARC uses four NIF beamlines to produce eight beamlets to create a sequence of eight images of an imploding fuel capsule using backlighting targets and diagnostic instrumentation. ARC employs a front end that produces two pulses, chirps the pulses out to 2 ns, and then injects the pulses into the two halves of each of four NIF beamlines. These pulses are amplified by NIF pre- and main amplifiers and transported to compressor vessels located in the NIF target area. The pulses are then compressed and pointed into the NIF target chamber where they impinge upon an array of backlighters. The interaction of the ARC laser pulses and the backlighting material produces bursts of high-energy x-rays that illuminate an imploding fuel capsule. The transmitted x-rays are imaged by diagnostic instrumentation to produce a sequence of radiograph images. A key component of the success of ARC is the automatic alignment system that accomplishes the precise alignment of the beamlets to avoid damaging equipment and to ensure that the beamlets are directed onto the tens-of-microns scale backlighters. In this paper, we describe the ARC automatic alignment system, with emphasis on control loops used to align the beampaths. We also provide a detailed discussion of the alignment image processing, because it plays a critical role in providing beam centering and pointing information for the control loops.

Keywords: Optical alignment, pattern recognition, image processing, image analysis

1. INTRODUCTION

The Advanced Radiographic Capability (ARC)¹⁻³ at the National Ignition Facility (NIF)⁴⁻⁶ is a petawatt-class, short-pulse laser system designed to provide x-ray backlighting of NIF targets. At the ARC front-end, two pulses derived from a lock-to-clock mode-locked oscillator centered at 1053 nm are chirped to 2 ns. These pulses are amplified and spatially shaped in the ARC Injection Laser System (ARC-ILS). The pair of pulses is divided into four sets of two pulses (or beamlets) and injected into four NIF main amplifiers for a total of eight beamlets. After amplification by the NIF main laser amplifiers, the beamlets are directed into one of two vacuum compressor vessels where they are compressed. The beamlets are directed out of the compressor vessels and focused into the NIF target chamber where they impinge upon an array of backlighters. (A very small fraction of the energy in a beamline is diverted from a compressor vessel to a diagnostic package where spatial, temporal and energy characteristics of the beamlets are analyzed.) The interaction of the ARC laser pulses and the backlighting material produces bursts of high-energy x-rays that illuminate an imploding fuel capsule. The transmitted x-rays are imaged by diagnostic instrumentation to produce a sequence of eight x-ray images displaying the progression of a fuel capsules compression.

Send correspondence to Randy S. Roberts: roberts38@llnl.gov

This work performed under the auspices of the U.S. Department of Energy by Lawrence Livermore National Laboratory under Contract DE-AC52-07NA27344. LLNL-CONF-674442.

The automated alignment capability of ARC is a critical part of the system. It provides a reliable, robust and efficient means to align optical elements to ensure safe and optimal operation of ARC. Although ARC is integrated into the NIF laser architecture, the technique to align ARC differs from that used to align NIF in several respects. One unique aspect of ARC is the use of pilot beams to perform alignment. ARC pilot beams are independent of NIF alignment light sources, thereby allowing ARC to be aligned in parallel with NIF. Another unique aspect of ARC alignment is the use of the Centering and Pointing System (CAPS), an optical device that provides simultaneous centering and pointing measurements on one camera relative to a single fiducial.⁷

Yet another unique aspect of ARC alignment is that it is designed to have some alignment cameras removed during high neutron yield shots to minimize damage to the cameras.⁸ This requirement led to placement of permanent reference fiducials, such as annuli and cross-hairs, along the path of pilot beams used for alignment. The interaction of the pilot beam and these fiducials creates diffraction patterns that contain both reference and beam locations (i.e., pixel coordinates) when imaged on a CCD camera. When a camera is removed and then replaced, the reference location does not need to be re-acquired through a calibration procedure. Moreover, in the alignment of NIF beamlines, a reference image is typically acquired followed by separate acquisition of a beam image. Since ARC alignment imagery typically has both reference fiducials and an alignment beam in the same image, the image processing associated with ARC alignment is often more complex than image processing associated with NIF alignments.

From a software point of view, ARC alignment is an extension of NIF alignment.⁹ NIF alignment software is designed to align all beamlines in parallel, and this characteristic is inherited by ARC. Both ARC and NIF alignment loops are developed from the same software base, and share a common structure. Alignment loops implement feedback structures needed to manipulate mirrors to center and point beams along a beampath. Image processing is an important component of alignment loops in that beam centroids and reference locations are found on imagery from CCD cameras strategically placed along the beam path. Beam centroid and reference locations are provided to the alignment loop to reposition mirrors and bring the optical path into alignment.

We begin by describing the characteristics of the alignment loops used in ARC (and NIF). Next, the ARC beampath is described, beginning with the ARC Front End and ARC-ILS. Although the ARC-ILS has several alignment loops and interesting image processing problems,¹⁰ space limitations preclude a discussion in this paper. Instead, we focus on alignment of the beampaths in the ARC Target Area (ARC-TA) segment. This area contains several alignment paths that contain challenging image processing problems. We describe the alignment loops and the illustrate alignment imagery and fiducials associated with the loops.

2. ALIGNMENT LOOPS

Automated alignment of the ARC (and NIF) is accomplished through execution of a sequence of control loops that center and point beams along beampaths.^{11,12} A block diagram of an alignment loop is illustrated in Figure 1. This loop can be used for either centering or pointing a beam, depending on whether the near- or far-field of the beam is imaged on a CCD camera. Essentially, a reference location (a pixel coordinate on a CCD array) and beam centroid (another pixel coordinate) are estimated using image processing algorithms, and the control loop manipulates mirror pairs to steer the beam centroid towards the reference location. The loop iterates until the distance between the beam centroid and reference location converges to within a tolerance on a CCD array as scaled to millimeters for centering loops or milliradians for pointing loops.

As illustrated in Figure 1, after the start-at-setpoint check is completed, the loop reserves and configures all of the devices that it will need to complete the alignment. Device reservation and configuration are performed by the Component Mediation System (CMS). A device reservation allows access to a device by only the reservation holder (e.g., an alignment loop), and locks out all other users (e.g., another alignment loop). Devices used by a loop include light sources, shutters, mirror motors and similar apparatus used for the alignment. The CMS provides a scripting mechanism whereby all the devices used in an alignment loop are listed and grouped into blocks of operations that can be performed in parallel. The CMS reservation system provides a means to avoid device conflicts when running many alignment loops in parallel.

After the device reservations are in place, the CMS configures the devices that are required by the loop for the alignment. Device configurations are managed through setpoints. A setpoint captures the possible states of

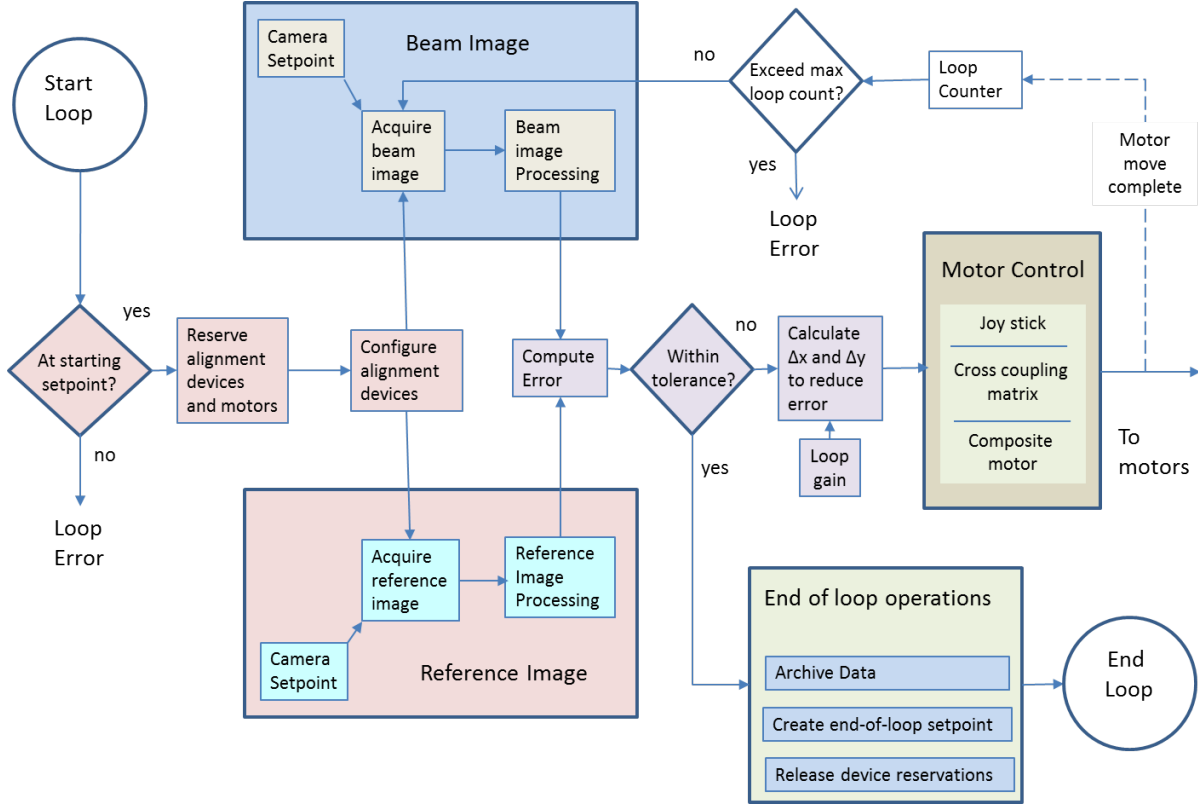


Figure 1. Schematic of a NIF and ARC control loop.

a device, such as the open or closed position of a beam shutter, the step counts on a motor, or camera attributes such as the integration time, orientation of the image, size of the image, and how the image is cropped. The CMS can create, delete or command devices to change states to predefined setpoints. The latter operation is typically used when the CMS configures devices for alignment.

After the devices used by the alignment loop have been reserved and configured, imagery is collected of a reference beam and the beam to be aligned by CCD cameras arranged along the beam path. CCD cameras used in the ARC alignment are size 1392×1040 pixels and 12-bits deep. For ARC, cameras near the NIF target chamber are designed to be removed after alignment to prevent damage caused by high neutron flux. References for loops that use these cameras are mounted separately from the cameras. This allows cameras to be removed and replaced without recalibration to find a reference location.

An alternative alignment loop configuration is to provide the loop with a predetermined pixel coordinate as the reference location. In this configuration, the reference location is determined when the loop is commissioned. It has the advantage of simplifying the control loop structure, and eliminating potential errors in the image processing associated with a reference image. However, if the CCD cameras are removed to prevent degradation due to neutron damage, then the reference location must be determined each time the camera is re-installed for a new shot—a potentially time consuming operation.

After collection of the reference and beam imagery, the imagery is processed by algorithms that extract fiducial information to determine the reference location and the location of the centroid of the beam to be aligned. The distance in millimeters for a centering loop (or milliradians for a pointing loop) between the reference pixel and beam location is calculated using predetermined scaling factors. This error is compared to a tolerance, and if the error is within tolerance, then the loop successfully concludes after archiving loop output, releasing devices used by the loop and imagery, and creating end-of-loop setpoints for the next alignment operation. The control loop starts with an option to check that the previous loop has successfully completed (cf. Figure 1). This check is particularly important for pointing loops, as the beam must be centered before the pointing loop begins. Thus,

if a pointing loop is starting and the previous centering loop failed to complete, then the pointing loop will error out and require operator intervention.

If the error between the beam centroid and reference location exceeds the loop tolerance, then distances δx and δy are calculated to move the beam location closer to the reference location. Due to uncertainties and imperfections in the mechanisms that implement the loop, mirror positions are adaptively adjusted over several iterations to step the beam location to the reference location rather than using one move to close the error. Depending on the size of the error, coarse- and fine-gains are applied to the moves. This allows loops to converge rapidly without overshoot as the beam nears the reference location. If the loop fails to converge after a predetermined number of iterations, the loop errors and operator intervention is required to complete the alignment operation.

Although the beam movements appear as simple x - and y -direction moves on the CCD array, quite complex adjustments of mirrors are required to implement the move. A mirror is moved by stepper motors positioned on the back of the mirror to adjust the tip and tilt of the mirror. Four motors (tip and tilt motors on two mirrors), are required to implement a centering and pointing loop. Beam movements δx and δy on a CCD array need to be translated into coupled mirror movements. A software object called a joystick is used to interface between movement commands calculated by the loop and underlying motor movement software. A joystick appears to the loop (or an operator) as a device that performs x - and y -direction beam movements on a CCD array, while in reality it is a high-level interface to cross-coupled motor control software.

Joystick commands to move a beam in the x - or y -direction are sent to a data structure called a cross-coupling matrix. The cross-coupling matrix maps distances δx and δy on the CCD array into step counts that motors on pairs of mirrors must simultaneously move in order to accomplish the beam movement on the CCD array. A row of a cross-coupling matrix contains stepper counts for each motor in the mirror system, and the counts for each motor in the row have been adjusted to yield a net effect of moving the beam in the x - or y -direction on the CCD array. The counts are also scaled so that the movements are in units of millimeters for centering loops and milliradians for pointing loops. Elements of the cross-coupling matrix are computed off-line and stored for use by alignment loops. Collections of motors are grouped into a software object called a composite motor, and the cross-coupling matrix provides the composite motor with the step counts required to perform the requested beam movement.

3. BRIEF OVERVIEW OF THE ARC BEAMLINE

To set the context for a discussion of the ARC automated alignment, we begin with a brief description of the ARC beampath. From a control perspective the ARC beampath consists of three segments:^{9,13} 1) the ARC Front End, 2) the ARC Injection Laser System (ARC-ILS), and 3) the ARC Target Area (ARC-TA). From an automated alignment perspective, the ARC alignment system consists of two segments: the ARC-ILS and the ARC-TA. (There are no alignment loops in the ARC Front end at this time.) As previously mentioned ARC is a subsystem of the NIF laser system and is integrated into NIF beamline architecture. To set the context for the ensuing discussion, see Burkhart¹⁴ for an overview of the NIF laser alignment, Bowers¹⁵ for an overview of the NIF ILS, and the webpage *Short-Pulse Lasers*¹ for a description of the ARC architecture.

The ARC-Front End produces two chirped, 2 ns pulses, denoted as the A and B beamlets, which are compressible to one picosecond. The pulses are inputted to the ARC-ILS, which consists of several subsystems that perform various operations on the pulses. The first subsystem of the ARC-ILS contains a regenerative amplifier which amplifies the pulses. The second stage of the ARC-ILS expands the beamlets and shapes the beams into rectangular beams with apodized edges. The A and B beamlets are also combined into a single beam in this stage of the ARC-ILS, with each beamlet occupying a non-overlapping portion of a NIF beamline. Figure 2 illustrates the spatial arrangement of the A and B beamlets in a NIF beamline along with a NIF beam for comparison.

The beamlets are next amplified by a Multi-Pass Amplifier (MPA) and then directed into a four-way splitter located in the Pre-Amplifier Beam Transport System (PABTS). Optical trombones in the PABTS stagger the timing of each set of ARC beamlets into a time series of pulses. The output of each branch of the splitter is inputted into a NIF beamline. As a result of this processing, eight ARC pulses are produced, with A and B beamlets in a NIF quad (i.e., four NIF beamlines). For reference, these beamlines are denoted as B351, B352,

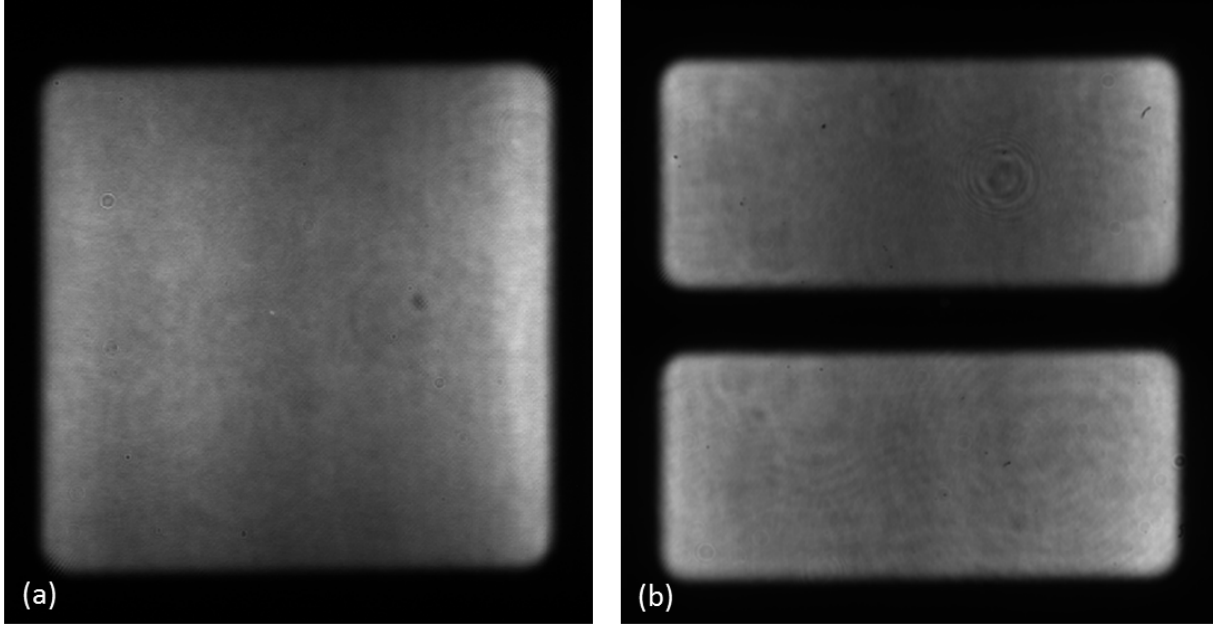


Figure 2. (a) NIF beam and (b) ARC Beamlets.

B353 and B354. The beamlets are amplified by NIF main amplifiers and transported to compressor vessels located in the NIF target area.

After amplification by the NIF main amplifiers, beamlines B351-B354 are diverted into two vacuum compressor vessels located in the NIF Target Area. Figures 3 and 4 provide complimentary schematics of the optical paths and alignment loops in the ARC-TA. Figure 3 shows the Transport path where ARC beamlets are directed into a compressor vessel by mirrors labeled AM1-AM4. (This figure depicts one compressor vessel while Figure 4 illustrates both compressor vessels.) The compressor vessels, denoted as CV1 and CV2, enclose gratings G1-G4 which compress beamlets back into laser pulses with duration on the order of picoseconds. The bulk of the energy in ARC beamlets is directed out of the compressor vessels by mirror AM5 towards the NIF Target Chamber. Along this path, the pulses are directed by mirrors AM6-AM8 towards the Target Chamber Center (TCC). Mirror AM7 is a parabolic mirror, which focuses the beamlets into spots with diameters on the order of 30 microns. Mirror AM8 points the pulses toward TCC where beamlets impinge upon an array of backlighters.

A small fraction of the beamlet energy in a selectable beamline is diverted out of a compressor vessel to a diagnostic table where instrumentation quantifies the spatial, temporal and energetic characteristics of the beamlets. Mirrors AM5 in CV1 and CV2 are partially transmitting, allowing 0.2% of each ARC beam to continue to DM1, as depicted in Figure 4. DM1 is mounted on a translation stage that allows it to move between the B351/B352 or B353/B354 beampaths. The ARC beamlets are reflected off of DM2 and DM3 and reach DM4, which rotates to select between beamlets in CV1 or CV2. Mirrors DM5, DM6 and DM7 are then used to direct beamlets in a single beamline to the diagnostic instrumentation package. In the diagnostic package, additional mirrors direct the beamlets to various instruments and the alignment cameras.

4. ALIGNMENT LOOPS IN THE ARC-TA SEGMENT

Alignment of the diagnostic path is accomplished with three small-diameter pilot beams at wavelengths 1053 nm and 980 nm. The 980 nm pilot beam represents the full beam aperture whereas each of the two 1053 nm pilot beams represents a sub-aperture (beamlet). These pilot beams are injected just below the main beam path in the compressor vessels. The two 1053 nm pilot beams are injected into the A beamlet and B beamlet compressor gratings and propagate towards AM5, whereas the single 980 nm beam does not interact with the compressor gratings and is directed to AM5 immediately after injection. The reason for pilot beams at different wavelengths is that mirrors to the diagnostic table are designed to reflect light at 1053 nm, the center wavelength of an

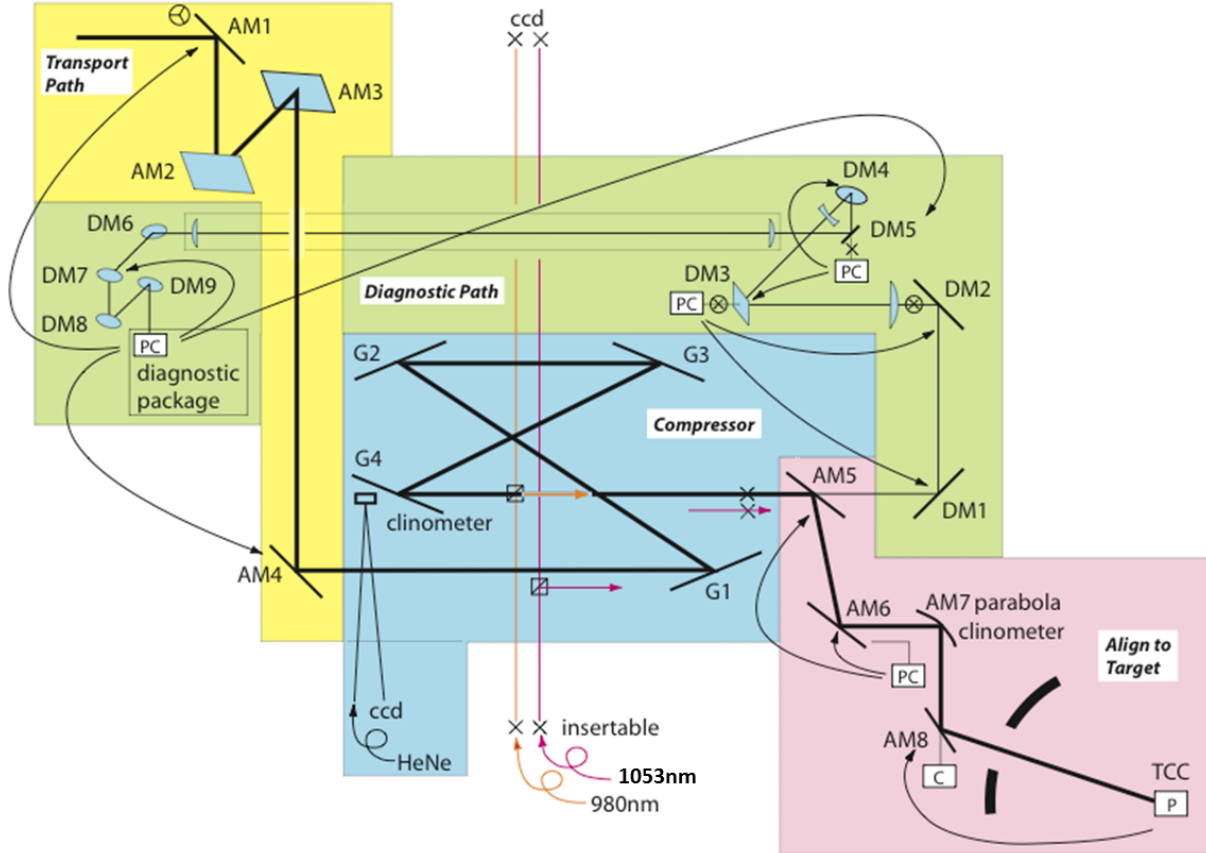


Figure 3. Schematic of the control loops in the ARC-TA segment. The boxes labeled 'PC' indicate the locations of the pointing and centering cameras, and the arrows emanating from these boxes indicate the mirror pairs that form the pointing and centering loops with those cameras.

ARC beamlet. These mirrors are coated to partially transmit 980 nm light, enabling propagation of a pilot beam to fiducials and cameras along the diagnostic beam path. Since the 1053 nm pilot beams propagate through the compressor vessel, and then to the diagnostic path, they also serve to indicate whether the gratings have become misaligned by observing the beams at the diagnostic table. The bottom of the AM5 mirror is uncoated and transmits greater than 90% of each pilot beam to the DM1 mirror on the diagnostic path. These pilot beams illuminate alignment references positioned at surveyed locations along the beam path. The cross-hairs and apertures impose patterns on the intensity profiles of the pilot beams which serve as reference fiducials.¹⁶

Figure 3 shows a schematic of the alignment loops in the ARC Target Area (ARC-TA) for one of the two ARC compressors. This figure depicts the four alignment paths in the ARC-TA: 1) the transport path into the ARC compressor vessel, 2) the compressor vessel, 3) the path to diagnostic instrumentation, and 4) the path to the NIF target chamber. Figure 3 denotes the pointing and centering CCD cameras for the loops on these paths as boxes labeled PC (for pointing and centering). These cameras are located behind mirrors DM3, DM5 and on the diagnostic package. Arrows emanating from these boxes indicate the mirror pairs used by these cameras to form alignment loops. For example, the centering and pointing cameras behind DM3 use mirrors DM1 and DM2 to center and point the beam into DM3. As another example, the centering and pointing cameras in the diagnostic package use mirrors AM1 and AM4 to center and point beams into a compressor vessel. We begin by describing the alignment path to the diagnostic instrumentation, as this path is shared by both compressor vessels.

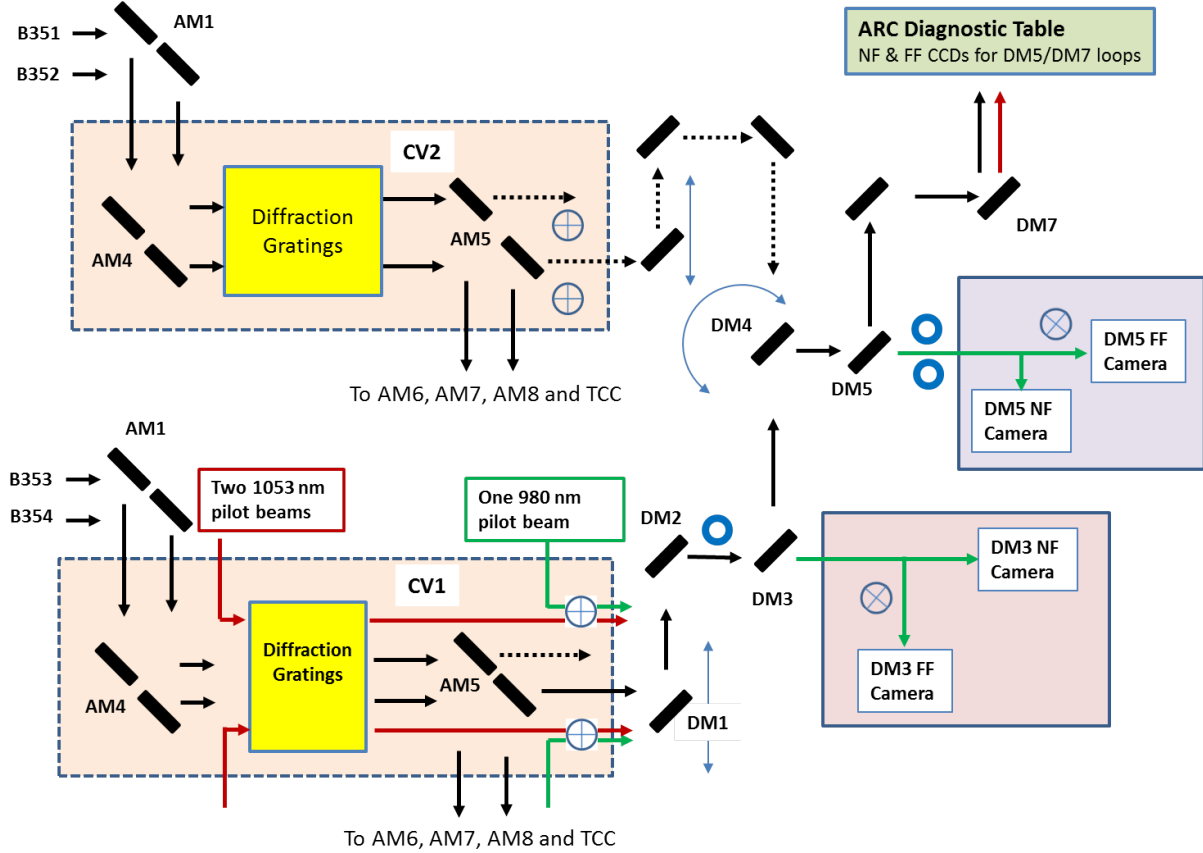


Figure 4. Schematic of the ARC diagnostic path. Alignment fiducials are denoted as circles near the beam paths that are either open (an annulus), or contain a 'x' or '+' symbol indicating a cross-hair. To avoid diagram clutter the DM3 near-field and far-field camera enclosure and pilot beams are only illustrated for the lower compressor vessel.

4.1 Path to diagnostic package

The first loop on the diagnostic path directs beamlets into the calorimeter package behind DM3 (see Figure 4). Centering and pointing along this portion of the diagnostic path is accomplished using mirror pairs DM1 and DM2. The near-field (centering) image is formed by the diffraction pattern caused by the AM5 '+' cross-hair and an annulus positioned in the 980 nm pilot beam path between the DM2 and DM3 mirrors, and is imaged by the centering camera behind DM3. This image is shown in Figure 5a, where a red-colored outline of the reference annulus has been superimposed on the diffraction pattern. The center of the annulus is the reference fiducial, and the center of the diffraction pattern is the beam location. The centering loop manipulates mirrors DM1 and DM2 to align the beam to the reference.

The far-field (pointing) image is formed by the '#' diffraction pattern from the AM5 '+' cross-hair and an 'x' shaped cross-hair behind DM3. This image is shown in Figure 5b, which shows the in-focus 'x' superimposed on the diffraction pattern from the AM5 cross-hair. The alignment loop manipulates the DM1 and DM2 mirrors to position the 'x' shadow on the center of the diffraction pattern.

The next portion of the diagnostic path directs beamlets into mirror DM5. Centering and pointing of the beam is performed by mirrors DM3 and DM4. As indicated in Figure 4, DM3 mirrors are associated with each compressor vessel, but a single DM4 rotates to select between CV1 and CV2. An annulus is positioned beneath DM5 for the 980 nm pilot beam from each compressor vessel. The pilot beam from the compressor selected by DM4 is imaged for the DM3/DM4 centering loop and is shown in Figure 6a. At this point, the diffraction pattern from the cross-hair under AM5 is minimal, and the loop aligns the centroid of the beam with the center of the annulus. The image processing algorithm for this loop is described in a paper by Roberts et al.¹⁶ The

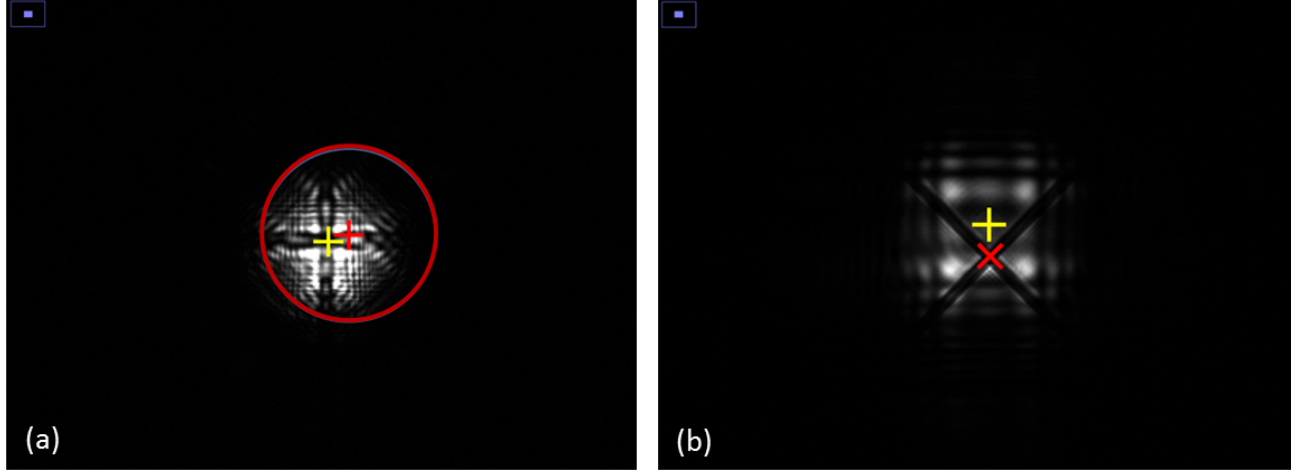


Figure 5. (a) Near-field image of the DM2/DM3 centering loop and (b) Far-field image of the DM2/DM3 pointing loop. The centering loop aligns the center of the diffraction pattern (a yellow '+') with the center of the annulus (a red '+'). (The red circle indicates the edge of the annulus, which is difficult to see in this image.) The pointing loop aligns the center of the diffraction pattern (a yellow '+') with the center of the 'x' cross-hair (a red 'x').

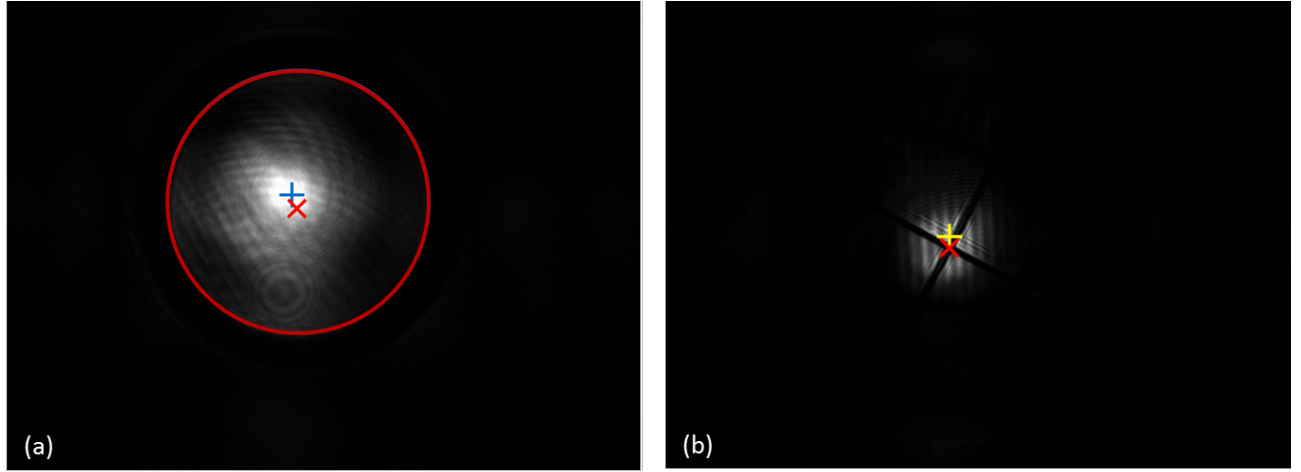


Figure 6. (a) Near-field image of the DM3/DM4 centering loop and (b) Far-field image of the DM3/DM4 pointing loop. The centering loop aligns the center of the diffraction pattern (a blue '+') with the center of the annulus (a red 'x'). (The red circle indicates the edge of the annulus, which is difficult to see in this image.) The pointing loop aligns the center of the diffraction pattern (a yellow '+') with the center of the 'x' cross-hair (a red 'x').

pilot beam and pointing reference, a \times -shaped cross-hair, are imaged on the pointing camera behind the DM5 mirror, and this image is shown in Figure 6b.

The final stage of the diagnostic path steers beamlets into the ARC diagnostic package using mirrors DM5 and DM7, as imaged with near- and far-field CCD cameras in the diagnostic package. The near-field image for the centering loop is shown in Figure 7a, and the far-field image is shown in Figure 7b. Alignment is performed using the 1053 nm pilot beams, which appear as very small (25×25 pixel) patterns on the near-field camera. The centering loop manipulates DM5 and DM7 to steer the pattern to a pre-determined reference pixel determined by the reference mask used in the AM1/AM4 centering loop. The image processing for the DM5/DM7 centering loop is described in a paper by Roberts et al.¹⁶ Although 1053 nm pilot beams appear in the near-field image from both halves of the selected beam, the alignment loop only processes one at a time. Thus, the DM5/DM7 centering loop aligns the A beamlet and verifies that the B beamlet is within a tolerance of its reference location.

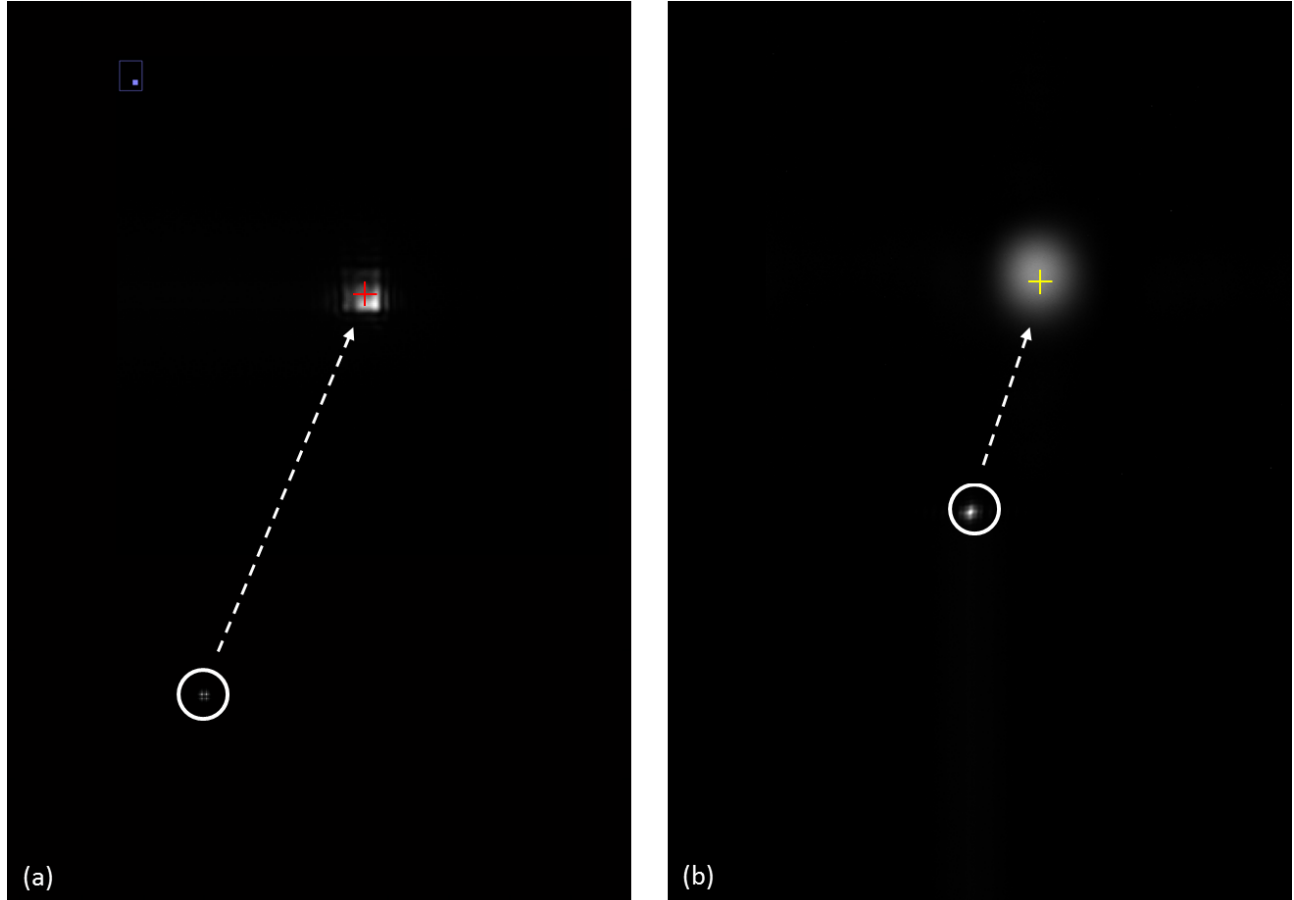


Figure 7. (a) Near-field image of the DM5/DM7 centering loop (greatly enlarged) for the 'A' beamlet and (b) Far-field image of the DM5/DM7 pointing loop (also greatly enlarged) for the 'A' beamlet. The centering loop aligns the center of the diffraction pattern, denoted with a red '+', with the corresponding 1053 nm spot for the 'A' beamlet on the AM1/AM4 reference mask as shown in Figure 8a. The pointing loop aligns the centroid of the beam, shown as a yellow '+' with a pixel location found from the AM1/AM4 reference mask.

The far-field image for the DM5/DM7 loop is shown in Figure 7b. It is essentially a Gaussian spot on the pointing camera and is accurately aligned to a pixel location pre-defined by the reference mask used in the AM1/AM4 pointing loop. Like the centering loop, the A beamlet is aligned first and the B beamlet is then checked against its tolerance.

4.2 Transport path to the Compressor Vessels

The transport path into the compressor vessels uses mirrors AM1 and AM4, which provide pointing and centering based on imagery collected at the diagnostic package. The references for the pointing and centering loops are pixel locations, and these locations are determined by a reference mask on the diagnostic table which is illuminated by a laser also on the table. Figure 8a shows an image of the reference mask as it appears on the near-field camera. The image processing algorithm estimates the centroid of the two rectangular regions and also the centroids of the three spots above and below the rectangular regions. The locations of these small spots mark the positions where the 980 nm pilot beam (center) and two 1053 nm pilot beams (straddling the 980 nm beam spots) should appear. The row of pilot beam spots on the bottom of the image is for compressor vessel CV1, and the row of spots on the top is for compressor vessel CV2.

An image of the beam pattern used for the AM1/AM4 centering loop is shown in Figure 8b. It is generated by a mask inserted in the ARC-ILS unit prior to the NIF main amplifier. The image processing for the centering

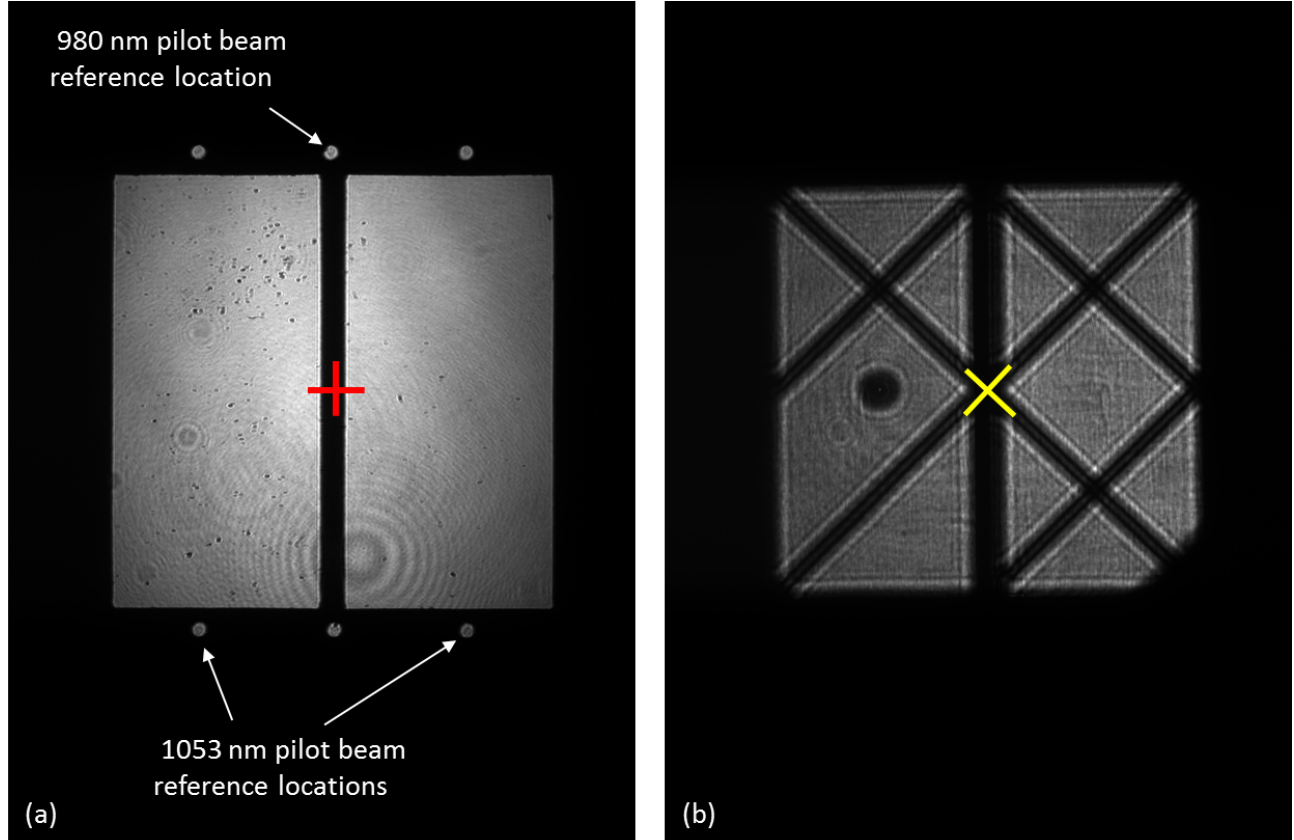


Figure 8. (a) AM1/AM4 reference mask as it appears on the ARC diagnostic package and (b) AM1/AM4 centering mask as it appears on the ARC diagnostic package. The centroid of the two large rectangular regions (a red '+') is the reference location for the AM1/AM4 centering loop, and these mirrors are manipulated to align the yellow 'x' in the centering mask with this location. The pilot beam reference locations are the locations where the near-field images of the pilot beams should appear when aligned.

loop estimates the center of the cross pattern that spans the A (right) and B (left) beamlets in the mask.¹⁷ This location is denoted by the yellow 'x' in the figure. Mirrors AM1 and AM4 are then manipulated to move the fiducial to the location of the reference pixel (within a tolerance). The AM1/AM4 pointing loop positions the far-field gaussian spot of the ARC-ISP light source onto the far-field reference pixel, which is determined by the AM1/AM4 reference mask centroid in the far-field.

4.3 Compressor vessel alignment verification

Beamlet compression is achieved with a sequence of four gratings, and the orientation of these gratings must be verified before each use of ARC. Verification of the positions of the gratings is accomplished with loops that estimate the positions of pilot beams retro-reflected from mirrors positioned on the back of the grating mount. A full description of the verification method and image processing algorithm for the compressor gratings is found in the paper by Roberts et al.¹⁸

4.4 Path to NIF Target Chamber

ARC beamlets are directed out of the compressor vessel with mirror AM5, and redirected into AM7 by AM6. Mirror AM7 is a parabolic mirror and is used to focus the ARC beamlets onto backlighters in the NIF target chamber. Centering and pointing into AM7 is accomplished with mirrors AM5 and AM6 using a unique optical system called CAPS (Centering and Pointing System).⁷ CAPS is designed to provide both centering and pointing optics in a single unit for the beam passing through the CAPS. It is a very compact device, and is used in the

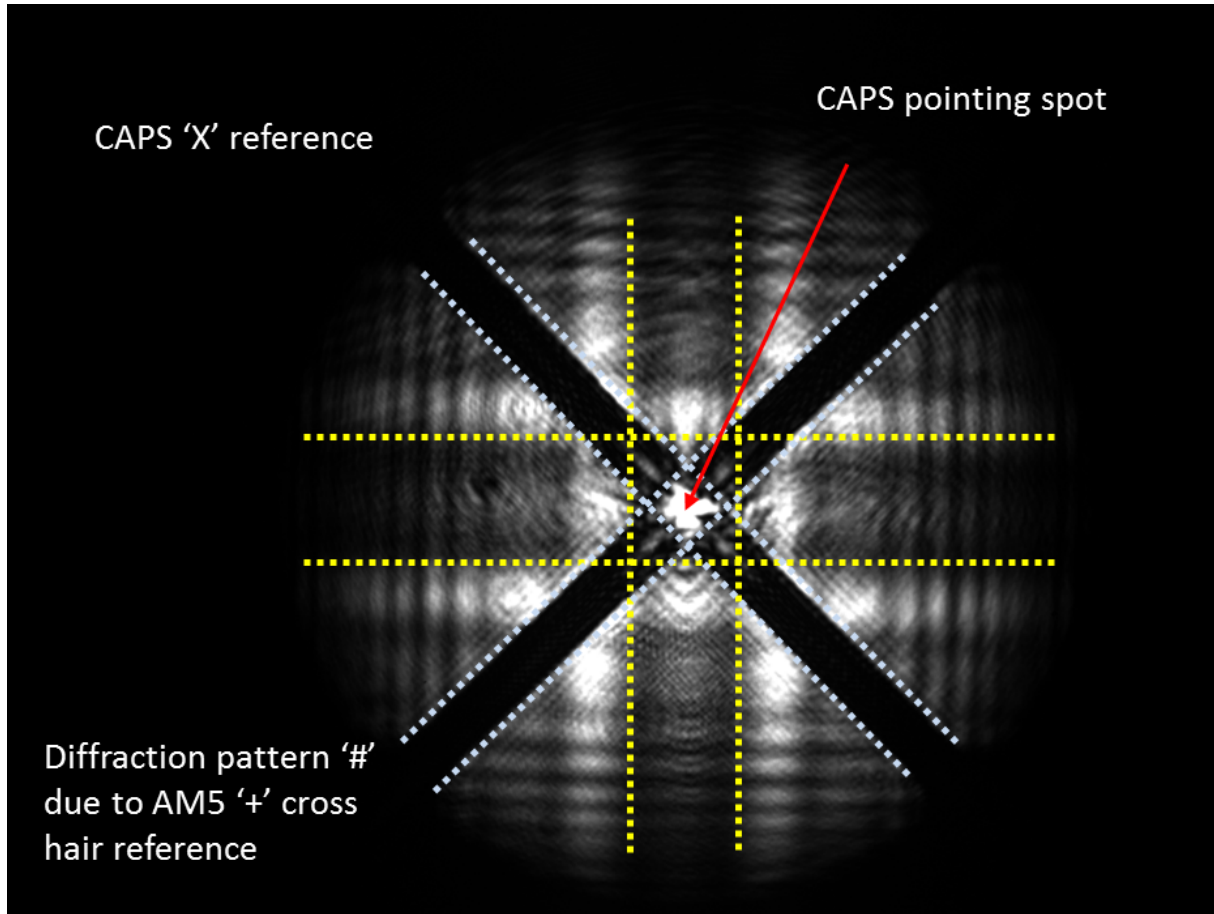


Figure 9. Annotated CAPS image.

AM5/AM6 loops due to size constraints at this point in the ARC beam path. An annotated image from the CAPS is shown in Figure 9.

The AM5, AM6 and AM7 mirrors manipulate the entire beam aperture and affect both sub-apertures identically (common-mode for the sub-apertures). This forces the decision to align with either the A or B sub-apertures (or and average of the two). With this in mind, the decision was made to center and point the A beamlet, and then verify the centering and pointing of the B beamlet. The alignment process consists of first using image processing to return the center of the 'x' (the centering reference) and then the center of the AM5 + cross-hair which becomes a '#'-shaped diffraction pattern. The center of the CAPS 'x' is fixed in the image, and the center of the '#' is movable via AM5 and AM6. These mirrors are manipulated to position the center of the '#' on the center of the 'x'. The centering of the B beamlet is then verified to be within its tolerance, and the alignment fails if the centering is out of tolerance. This situation indicates an off-normal alignment condition such as pointing drift between the compressor gratings or the pilot beams, or some other undesirable condition.

Pointing the A beamlet begins by decreasing the camera integration time to emphasize the pointing spot, which is typically much brighter than the rest of the diffraction pattern. Image processing is then applied to return the centroid of the pointing spot. The AM5/AM6 mirrors are then adjusted to set the pointing spot to the combined centers of the 'x' and '#' patterns. Verification of the B beamlet pointing is conducted in the same manner but without mirror adjustment. The image processing algorithms that extract the features and estimate the locations of fiducials are described in the paper by Leach et al.¹⁹

5. SUMMARY

We have described the alignment loops used in the ARC-TA segment. These loops have been deployed, tested and are being used to align this segment. Our discussion began with a description of the alignment loops used in the ARC. The loop description is very general, and loops like the one described here are used throughout NIF to align various segments of the laser. The Component Mediation System (CMS) is a critical part of an alignment loop, as it provides a mechanism for reserving and configuring devices used in the alignment. The general form of an alignment loop also requires both reference image and beam image in order to align a beam path.

Alignment loops in the ARC-TA are unique from NIF loops in that offset pilot beams and fiducials in their paths are used to form a single alignment image that contains both the reference and beam locations. This arrangement allows cameras in the ARC-TA to be removed during high-yield shots as a neutron-damage mitigation step. Image processing for these loops is often more complex than that used in NIF loops and we provide illustrations of the alignment imagery and fiducials that must be determined by the image processing. We also described an alternative loop structure in which a predetermined reference location (i.e., a pixel location on the alignment CCD camera array) is provided to the loop using a-priori knowledge of the desired alignment. This technique is used in several of the ARC-TA loops, and can also be used where the neutron yield does not cause damage to alignment cameras.

REFERENCES

1. “Short-pulse lasers.” <https://lasers.llnl.gov/science/photon-science/arc>. Accessed 8 July 2015.
2. C. Barty, M. Key, J. Britten, R. Beach, G. Beer, C. Brown, S. Bryan, J. Caird, T. Carlson, J. Crane, *et al.*, “An overview of LLNL high-energy short-pulse technology for advanced radiography of laser fusion experiments,” *Nuclear Fusion* **44**(12), p. S266, 2004.
3. J. Crane, G. Tietbohl, P. Arnold, E. Bliss, C. Boley, G. Britten, G. Brunton, W. Clark, J. Dawson, S. Fochs, *et al.*, “Progress on converting a NIF quad to eight, petawatt beams for advanced radiography,” in *Journal of Physics: Conference Series*, **244**(3), p. 032003, IOP Publishing, 2010.
4. G. H. Miller, E. I. Moses, and C. R. Wuest, “The National Ignition Facility,” *Optical Engineering* **43**(12), pp. 2841–2853, 2004.
5. E. I. Moses, “Ignition on the National Ignition Facility: a path towards inertial fusion energy,” *Nuclear Fusion* **49**(10), p. 104022, 2009.
6. E. I. Moses, “The National Ignition Facility and the National Ignition Campaign,” *Plasma Science, IEEE Transactions on* **38**(4), pp. 684–689, 2010.
7. M. C. Rushford, “Laser beam centering and pointing system,” Jan. 13 2015. US Patent 8,934,097.
8. A. A. Awwal, A. Manuel, P. Datte, M. Eckart, M. Jackson, S. Azevedo, and S. Burkhart, “Effects on beam alignment due to neutron-irradiated CCD images at the National Ignition Facility,” in *SPIE Optical Engineering+ Applications*, pp. 81340J–81340J, International Society for Optics and Photonics, 2011.
9. G. Brunton *et al.*, “The Advanced Radiographic Capability, a major upgrade of the computer controls for the National Ignition Facility,” in *Proceedings of the International Conference on Accelerator and Large Experimental Physics Control Systems (ICALPCS)*, pp. 39–42, 2013.
10. A. A. Awwal, R. R. Leach, R. S. Roberts, K. Wilhelmsen, D. McGuigan, and J. Jarboe, “Detecting objects with partial obstruction at the ARC split beam injector images at the National Ignition Facility,” in *SPIE Optical Engineering+ Applications*, pp. 92160E–92160E, International Society for Optics and Photonics, 2014.
11. K. Wilhelmsen, A. A. Awwal, D. Kalantar, R. Leach, R. Lowe-Webb, D. McGuigan, and V. M. Kamm, “Recent advances in automatic alignment system for the National Ignition Facility,” in *SPIE LASE*, pp. 79160O–79160O, International Society for Optics and Photonics, 2011.
12. K. Wilhelmsen, A. Awwal, G. Brunton, S. Burkhart, D. McGuigan, V. M. Kamm, R. Leach, R. Lowe-Webb, and R. Wilson, “2011 status of the automatic alignment system for the National Ignition Facility,” *Fusion Engineering and Design* **87**(12), pp. 1989–1993, 2012.

13. K. Wilhelmsen, E. Bliss, G. Brunton, B. Fishler, R. Lowe-Webb, D. McGuigan, R. Roberts, and Rushford, "Automatic alignment upgrade of Advanced Radiographic Capability for the National Ignition Facility," in *Proceedings of the International Conference on Accelerator and Large Experimental Physics Control Systems (ICALEPCS)*, pp. 1384–1387, 2013.
14. S. Burkhart, E. Bliss, P. Di Nicola, D. Kalantar, R. Lowe-Webb, T. McCarville, D. Nelson, T. Salmon, T. Schindler, J. Villanueva, *et al.*, "National Ignition Facility system alignment," *Applied Optics* **50**(8), pp. 1136–1157, 2011.
15. M. Bowers, S. Burkhart, S. Cohen, G. Erbert, J. Heebner, M. Hermann, and D. Jedlovec, "The injection laser system on the National Ignition Facility," in *Lasers and Applications in Science and Engineering*, pp. 64511M–64511M, International Society for Optics and Photonics, 2007.
16. R. Roberts, A. Awwal, R. Leach, M. Rushford, E. Bliss, and K. Wilhelmsen, "Image analysis for the automated alignment of the Advanced Radiography Capability (ARC) diagnostic path," in *Proceedings of the International Conference on Accelerator and Large Experimental Physics Control Systems (ICALEPCS)*, pp. 1274–1277, 2013.
17. R. R. Leach, A. Awwal, S. Cohen, R. Lowe-Webb, R. Roberts, T. Salmon, D. Smauley, and K. Wilhelmsen, "Advanced Radiographic Capability (ARC) ISP alignment mask fiducial pattern design and image processing," in *SPIE Optical Engineering+ Applications*, International Society for Optics and Photonics, 2015. forthcoming.
18. R. S. Roberts, E. S. Bliss, M. C. Rushford, J. M. Halpin, A. A. Awwal, and R. R. Leach, "Image analysis algorithms for the Advanced Radiographic Capability (ARC) grating tilt sensor at the National Ignition Facility," in *SPIE Optical Engineering+ Applications*, pp. 92160B–92160B, International Society for Optics and Photonics, 2014.
19. R. R. Leach, A. Awwal, E. Bliss, R. Roberts, M. Rushford, K. Wilhelmsen, and T. Zobrist, "Analysis of the confluence of three patterns using the Centering and Pointing System (CAPS) images for the Advanced Radiographic Capability (ARC) at the National Ignition Facility," in *SPIE Optical Engineering+ Applications*, pp. 92161Q–92161Q, International Society for Optics and Photonics, 2014.